COMPDYN 2011
3rd ECCOMAS Thematic Conference on
Computational Methods in Structural Dynamics and Earthquake Engineering
M. Papadrakakis, M. Fragiadakis, V. Plevris (eds.)
Corfu, Greece, 25–28 May 2011

SEISMIC STRENGTHENING OF THE HISTORIC CHURCH OF STs HELEN AND CONSTANTINE IN PIRAEUS

Constantine C. Spyrakos[1*], Panagiotis D. Kiriakopoulos[2], Eleni Smyrou[3]

Department of Civil Engineering, Earthquake Engineering Laboratory (LEE), National Technical University of Athens (N.T.U.A.), Zografos 15700, Athens, Greece

[1] Professor, Director of LEE *cspyrakos@central.ntua.gr*
[2] PhD candidate *pkiriakopoulos@teemail.gr*
[3] Researcher *smiroulena@gmail.com*

Key words: Masonry historic structure, Church retrofit, Seismic strengthening, Finite elements analysis, Ambient and laboratory structural and material testing

Abstract. *The Church of St. Constantine & Helen is located in the Municipal Theater square in Piraeus. It was constructed in 1882. A series of recent earthquakes, including the Athens 1999 earthquake, strained the temple and caused serious damages. These damages are mainly attributed to the absence of particular provisions to carry the earthquake loads. In order to evaluate the earthquake vulnerability of the church, a detailed study of the masonry structure was conducted in order to determine the mechanical properties, the building construction details and the current condition of the structure as well as its dynamic behavior through in situ and laboratory testing as well as through finite element analysis. Based on the results, strengthening and repair measures are proposed, using a combination of masonry consolidation techniques, fiber reinforced plastic materials (FRP) and steel tie rods.*

1 INTRODUCTION

Newly introduced materials and technology provide engineers with the ability to repair, reinforce and restore historic buildings with a more scientific, effective and less intrusive approach. The restoration process of a heritage building that has succumbed serious damage, should be based on a reliable assessment of its state of stress and deformation before and after the intervention. Such a process usually employs computer aided methods and arithmetic models; monumental and cultural heritage buildings are often analyzed with the finite element method (FE). The method uses a model that should simulate the actual behavior of the structure for both static and seismic loads. Therefore, it is imperative that the model is developed with data collected from in-situ and laboratory testing (geometry, crack pattern, material properties, etc.) in order to obtain realistic results that can be used for repair and strengthening of the structure. [1]

2 MONUMENT DESCRIPTION

2.1 General information

The Church of St. Constantine & Helen is located in the Municipal Theater square of Piraeus. Its construction begun in 1878 and ended in 1882. It is considered as one of the most majestic temples of Piraeus and was based on the blueprints of the architect John Lazarimos. Moreover, it is characterized by a capacity of 1200 people, its impressive bell-towers and a high dome. After the end of the construction, many prominent hagiographers and marble-sculptors undertook the decoration of the temple interior.

From an architectural perspective, the temple is a “domed basilica”. Its dome is carried on four concave triangular pendentives that serve to the transition from the circular base of the dome to its rectangular base. The weight of the dome passes through the pendentives to four massive piers at the corners. The length of the temple is 29m and the width is 23m. The total height of the temple is 23.4m with the dome and the bell towers being 7.2m and 8.6m high, respectively.

Figure-1: Front view of the temple

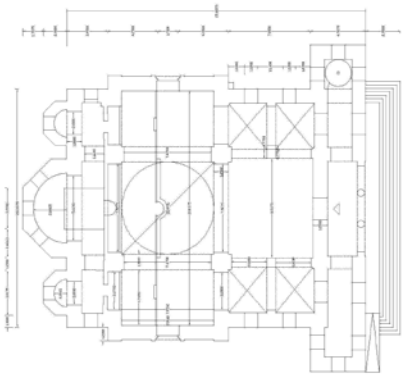

Figure-2: Plan view of the temple

2.2 Material and structural data of the church

2.2.1. Stones and mortar

At three characteristic locations of the church, the external cover of the masonry was removed at square surfaces of 50x50cm (Fig.5); two of them on masonry walls and the third on a pier. Subsequently, the stone strength was measured using a rebound hammer that was

calibrated. Based on these measurements, the compressive strength of stone was estimated to be:

$$f_{bc} = 30\text{MPa}$$

Mortar samples were analyzed at the laboratories of Chemical Engineering at NTUA. The analysis procedure included three steps: (a) Natural separation of mortar-stone, (b) X-Ray diffraction, see Figure 3 and (c) Thermal analysis TG-DTG, see Figure 4. The analysis showed that mortar is hydraulic lime with a compressive strength:

$$f_{mc} = 1\text{MPa}$$

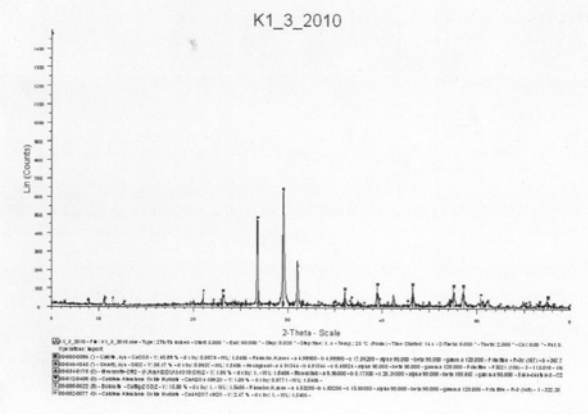

Figure-3: X-Ray analysis results

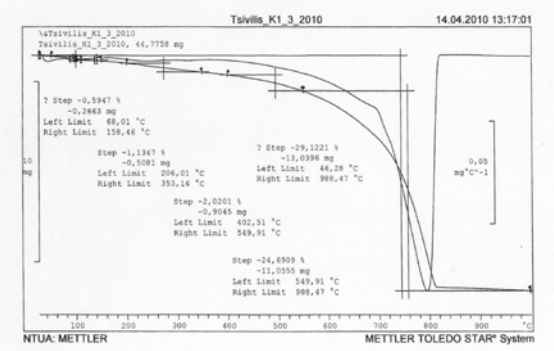

Figure-4: Thermal analysis results

2.2.2. Masonry wall type

In order to identify the transversal orientation of the materials constituting the masonry walls, drill cuttings were made and with the use of an endoscope the interior layers of the wall were inspected (Fig. 5-6). Results showed that the masonry walls are comprised of three layers. The external layers are stone of 25-30cm thickness. Moreover, the internal layer consists of solid mortar and small diameter stones.

Figure-5: Area without mortar cover

Figure-6: Inside the drill cutting

2.2.3. Masonry wall properties

In order to calculate the compressive strength of the stone masonry, the expression recommended by Tasios et. al. [2] was used:

$$f_{wc} = \frac{2}{3}\sqrt{f_{bc}} - a + \beta f_{mc} \quad (1)$$

where:
f_{bc} and f_{mc} is the compressive strength of stone and mortar, respectively, α is a reduction factor for masonry made of natural stone (α=1) and β is a factor that accounts for the contribution of mortar on the masonry wall strength (for stone masonry β is equal to 0.5).

According to bibliography, the tensile strength of masonry and Young's modulus were calculated with the aid of equations (2) and (3). The material properties are presented in Table-1.

$$f_{tc} = f_{wc}/10 \quad (2)$$

$$E = 1000\, f_{wc} \quad (3)$$

Material	Property	Value
Stone	Compressive strength	30 MPa
Mortar	Compressive strength	1 MPa
Stone masonry	Density	2200 kg/m^3
	Young's modulus	3150 MPa
	Poisson's ratio	0.16
	Compressive strength	3.15 MPa
	Tensile strength	0.315 MPa
Marble	Density	2600 kg/m^3
	Young's modulus	64200 MPa

Table-1: Material properties

3 MONUMENT PATHOLOGY

A series of recent earthquakes, including the Athens 1999 earthquake, strained the church and caused serious damage. These damages are mainly attributed to the fact that there are no special provisions in the building to protect it, in case of earthquake. In particular, cracks are located in many parts of the masonry wall, both external and internal and mainly in the intrados of the arcs.

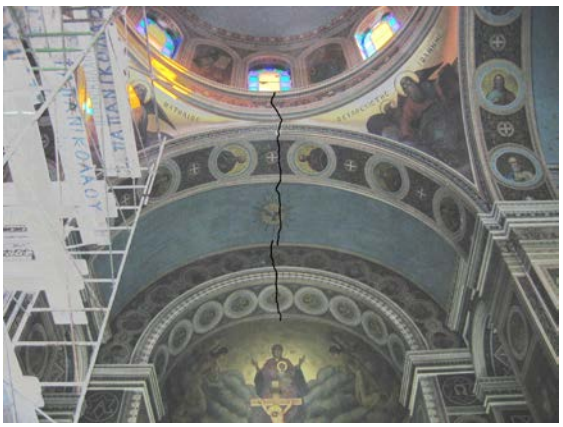

Figure-7: Sample crack at the east ceiling

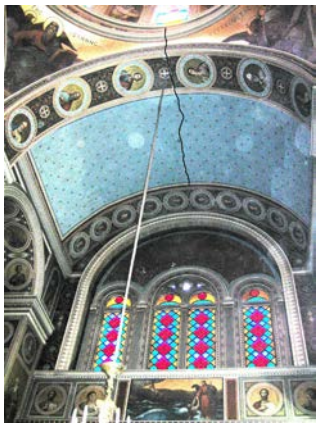

Figure-8: Sample crack at the south ceiling

Those with the largest width are located on the inner surface of the arcs, along longitudinal and transversal directions. Cracks were also developed at the triangular pendentives, which support the dome.

4 AMBIENT VIBRATIONS TESTS

To measure modes and natural frequencies of the church in its present state, ambient vibrations tests were conducted. In order to fulfill the task of the tests, there were measurements in two distinct positions, ground floor and dome level, along two directions. The results are presented in the following Tables (a) and (b) as they are obtained from the peaks in figures 9 and 10.

Mode	Modal Period (sec)	Damping Ratio (%)
1	0.372	4.5
2	0.273	3.3

(a)

Mode	Modal Period (sec)	Damping Ratio (%)
1	0.240	5.8

(b)

Table-2: Measurements at (a) transverse direction x-x’ and (b) longitudinal direction y-y’

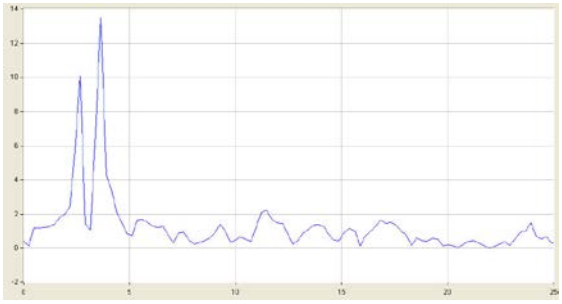

Figure-9: Deformation function at transverse direction x-x’

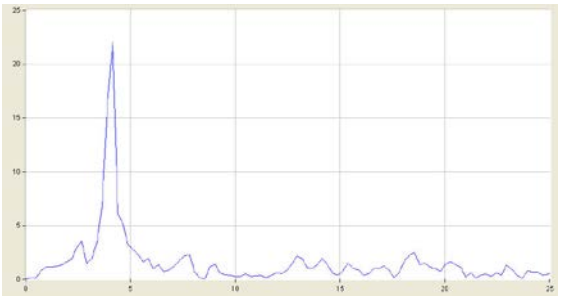

Figure-10: Deformation function at longitudinal direction y-y’

5 NUMERICAL ANALYSIS

5.1 Finite elements model

SAP2000 [3] finite element software was used to create and analyze the structure. The stone masonry and marbles were modeled by eight node solid elements with three degrees-of-freedom per node. Four-node shell elements were used to model the central dome. Two node-frame elements were used for the proper connection and collaboration of solid and shell elements [1]. The final model consists of 31055 solids, 2424 shells, 96 frame elements and 44204 nodes (Fig. 11-12).

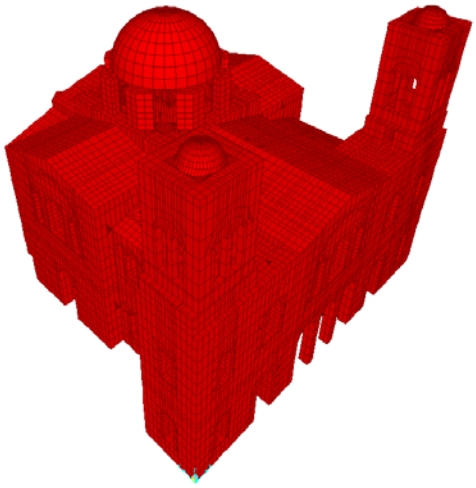

Figure-11: General view of the model

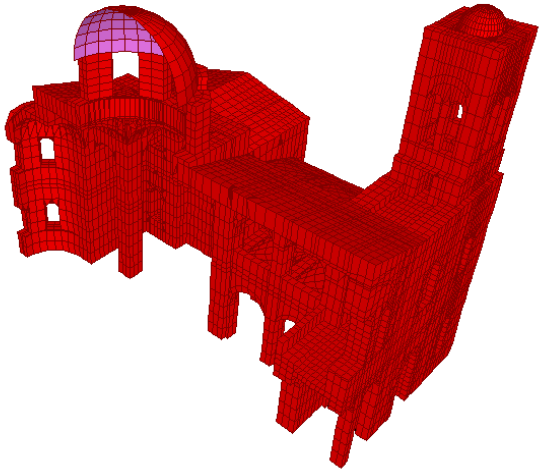

Figure-12: Section along the longitudinal direction

5.2 Response spectrum analysis

A response spectrum analysis was conducted. According to Eurocode 8-1 [4], the design spectrum Type-1 was used to calculate the seismic acceleration in both the horizontal and the vertical directions.

For the horizontal components of the seismic action the design spectrum, $S_d(T)$, is defined by the expressions (4)- (7):

$$0 \le T \le T_B : \; S_d(T) = a_g \cdot S \cdot \left[\frac{2}{3} + \frac{T}{T_B} \cdot \left(\frac{2,5}{q} - \frac{2}{3} \right) \right] \tag{4}$$

$$T_B \le T \le T_C : \; S_d(T) = a_g \cdot S \cdot \frac{2,5}{q} \tag{5}$$

$$T_C \le T \le T_D : \; S_d(T) \begin{cases} = a_g \cdot S \cdot \dfrac{2,5}{q} \cdot \left[\dfrac{T_C}{T} \right] \\ \ge \beta \cdot a_g \end{cases} \tag{6}$$

$$T_D \le T : \quad S_d(T) \begin{cases} = a_g \cdot S \cdot \dfrac{2,5}{q} \cdot \left[\dfrac{T_C T_D}{T^2} \right] \\ \ge \beta \cdot a_g \end{cases} \tag{7}$$

where T is the vibration period in secs, a_g = 0.16g is the design ground acceleration for type A ground, T_B = 0.15 is the lower limit of the period of the constant spectral acceleration branch, T_C = 0.5 is the upper limit of the period of the constant spectral acceleration branch, T_D = 2 defines the start of the constant displacement response range of the spectrum, S = 1.2 is the soil factor, η is the damping correction factor with a reference value of η = 1 for 5% viscous damping, q = 1.5 the behavior factor and β = 0.2 is the lower bound factor for the

horizontal design spectrum. For the vertical component of the seismic action the design spectrum $S = 1.0$, $T_B = 0.05$, $T_C = 0.15$, $T_D = 1.0$

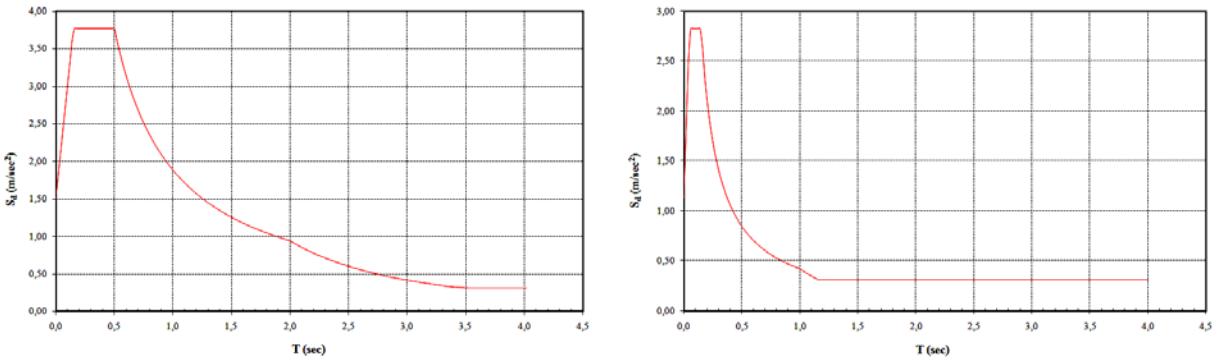

Figure-13: Design spectra for the horizontal and vertical seismic action

5.3 Analysis results

The results of modal analysis for the first three modes and the corresponding modal participating mass ratios are shown in Table-3. There is a good correlation between the measured and calculated modal periods which validates use of the model of the structure at least for static and small intensity dynamic loads.

Mode	Period (sec)	Ux	Uy	Uz	Rx	Ry	Rz
1st	0.320	0.728	0.00067	8.746E-07	0.00031	0.29906	0.2789
2nd	0.296	0.0003	0.776	1.139E-06	0.34906	0.00015	0.35204
3rd	0.228	0.032	0.00087	3.504E-07	0.00065	0.01385	0.10877

Table-3: Modal periods and participating mass ratios for displacement (U) and rotation (R)

The stresses at the transversal direction x-x' (S11) and at the longitudinal direction y-y' (S22) are shown in Fig. 14. With the deep blue (darkest color) are the areas where developed stresses are greater than the tensile strength of masonry. These areas are extensive and correspond to the areas where damages were observed at the temple.

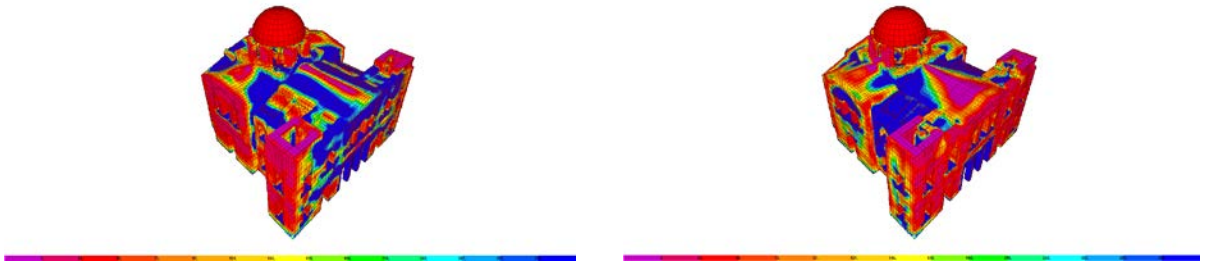

(a) (e)

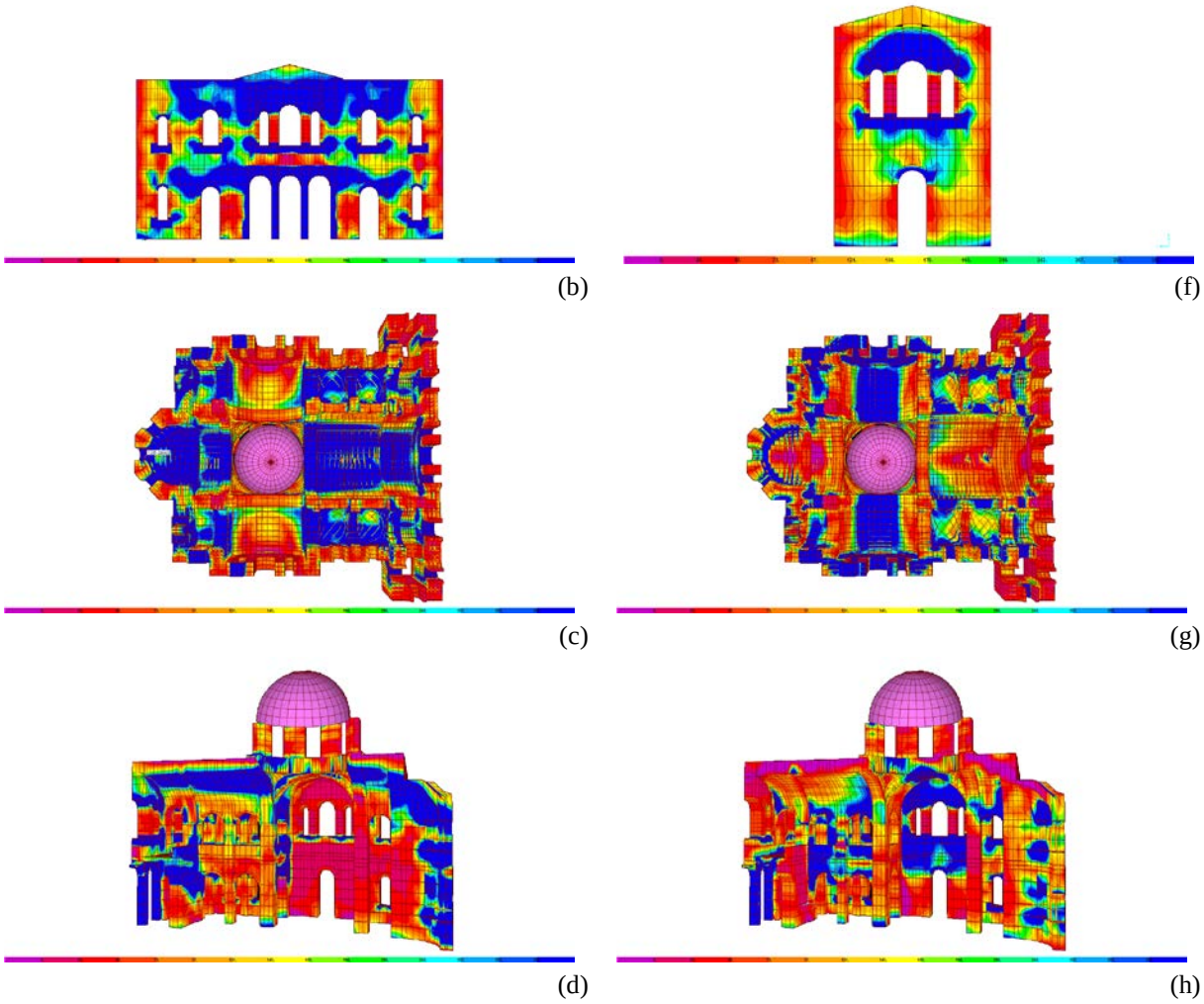

Figure-14: S11 (a-d) and S22 (e-h) stresses of the temple

It should be noted that this paper presents the first part of the analysis that was conducted for the historic structure. The second part presents a kinematic analysis as well as two displacement based analysis using frame as well as shell elements, respectively. Also, the second part elaborates on the correlation between the experiment and the analytical results and presents a comparison among the results of all three analyses.

6 REINFORCEMENT

According to the results of the analysis and the architectural- intervention restrictions imposed by the authorities that require minimum alteration of the structural configuration of the historic building and its painted walls, rehabilitation and strengthening of the church was based on a combined scheme using grout injections, CFRP and steel tie rods that complied with all limitations [5, 6]. The scheme is described in the following sections.

6.1 Grouting

The technique of grout injection in masonry through small holes drilled in the mortar at the exterior of the church walls will be used to consolidate the three leaf walls. Care will be taken to control the injection application so that the grout will not emerge on the interior surface of

the walls. The compressive strength of the masonry after consolidation, $f_{wc,s}$, is calculated from [7]

$$f_{wc,s} = f_{wc,0} + 0{,}31(V_{\text{inf}} / V) f_{gr}^{1{,}18} \quad (8)$$

where:

$f_{wc,0}$ the compressive strength before grout injection

V_{inf}/V ratio of grout volume to masonry volume

f_{gr} compressive strength of injected material

According to the international experience for seismic strengthening of three-leaf masonry walls, consolidation of the masonry walls can be accomplished with this technique. A compressive strength of 10 MPa was used in the analysis for the injected material in order to restrain failure in the grout of the consolidated wall.

6.2 Composite materials CFRP and stainless steel tie rods

According to the analysis, undertaking of the tensile stresses can be achieved by applying sheets of fiber carbon impregnated with epoxy resins on the upper exterior surface of the church (roof) as well as at parts of the interior surfaces of certain vaults that are not decorated with historic paintings. Specifically either three or two-plies of carbon fiber reinforced plastics (CFRP), with a carbon sheet thickness of 0.17 mm is selected. The mechanical properties of the carbon fiber are: modulus of elasticity E_c= 240 GPa, ultimate strength f_j= 3500 MPa.

Also two stainless steel tie-rods F430 with a diameter of 40mm should be placed at the upper part of the arches in the interior of the church. The mechanical properties of the tie-rods are: modulus of elasticity E_c= 200 GPa, yield strength f_y= 379 MPa, ultimate strength f_u= 552 MPa.

7 ANALYSIS OF STRENGTHED STRUCTURE

The results of modal analysis for the first three modes of the strengthened structure and the modal participating mass ratios are shown in Table-4.

Mode	Period (sec)	Ux	Uy	Uz	Rx	Ry	Rz
1st	0.250	0.74	0.00045	1.639E-06	0.00021	0.30279	0.28297
2nd	0.230	0.000085	0.77	1.171E-07	0.34847	0.000047	0.3621
3rd	0.180	0.02743	0.00298	5.506E-07	0.00191	0.01185	0.10544

Table-4: Modal periods and participating mass ratios for displacement (U) and rotation (R)

Figure-15: Placement of CFRP on the intrados of the arced ceiling

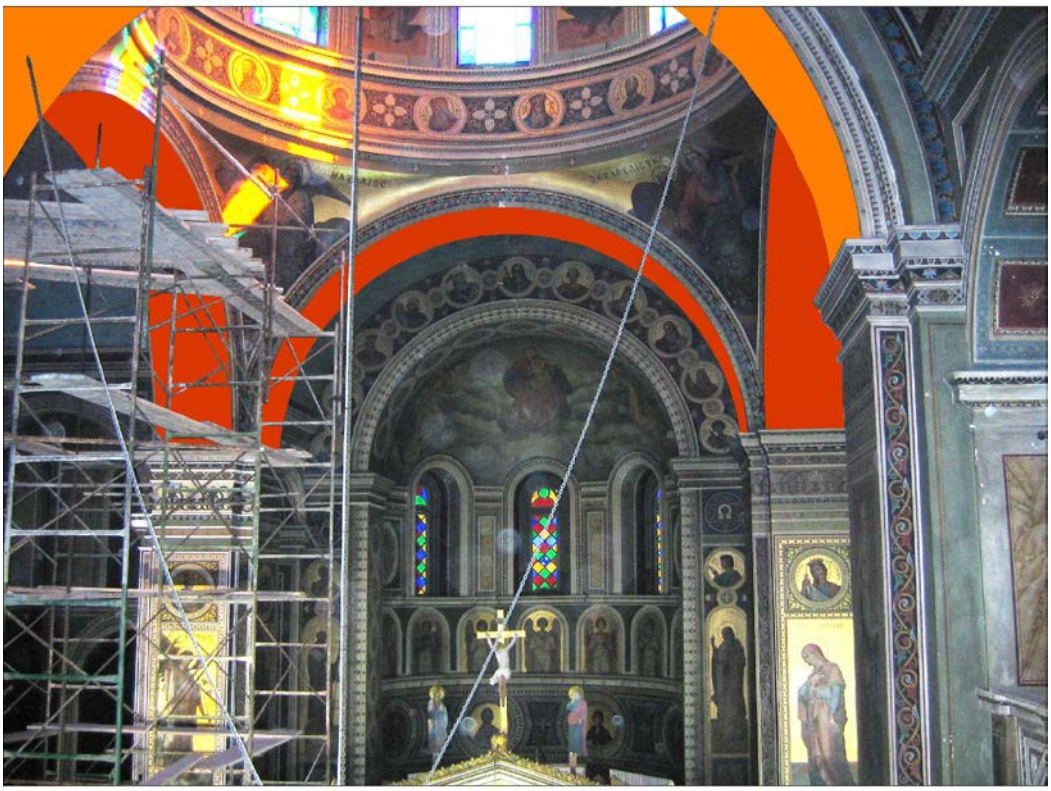

Figure-16: Placement of CFRP on the arcs of central dome

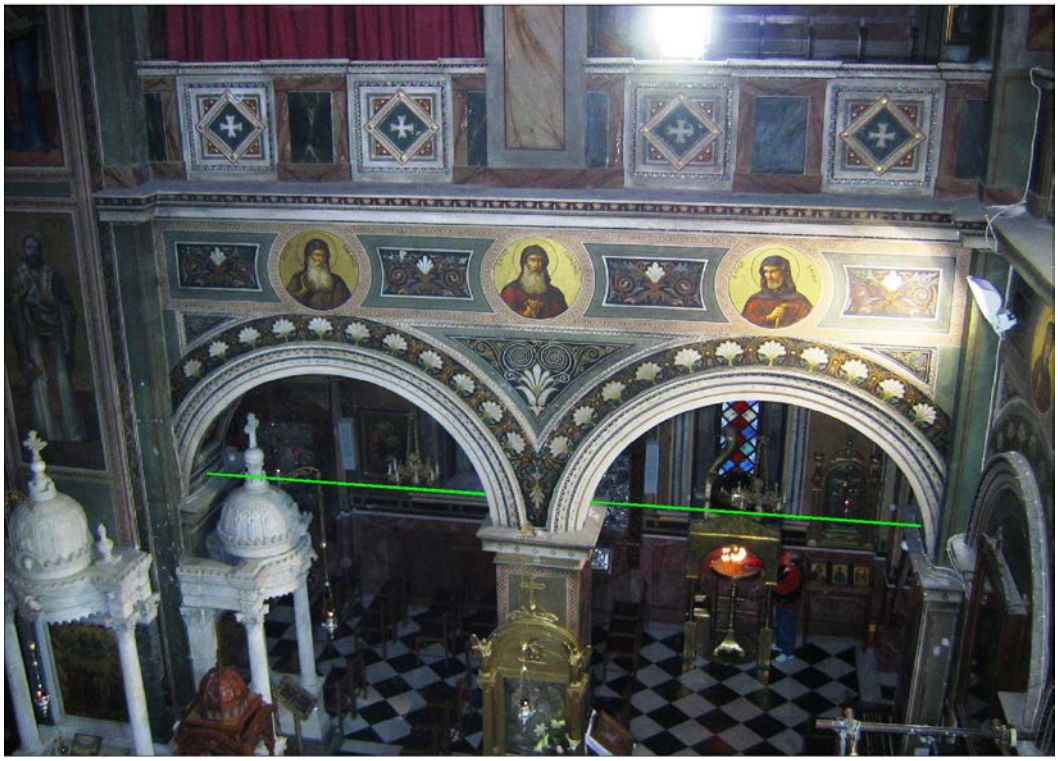

Figure-17: Placement of tie rods at arcs

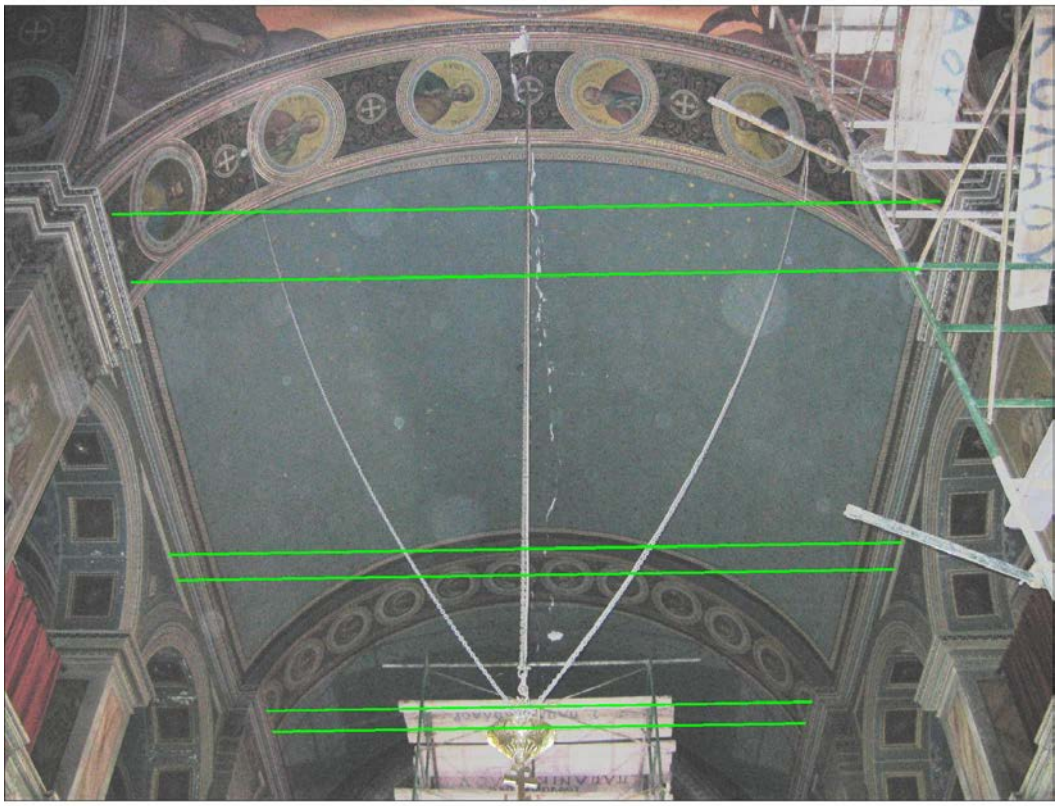

Figure-18: Placement of tie rods at the central arced ceiling

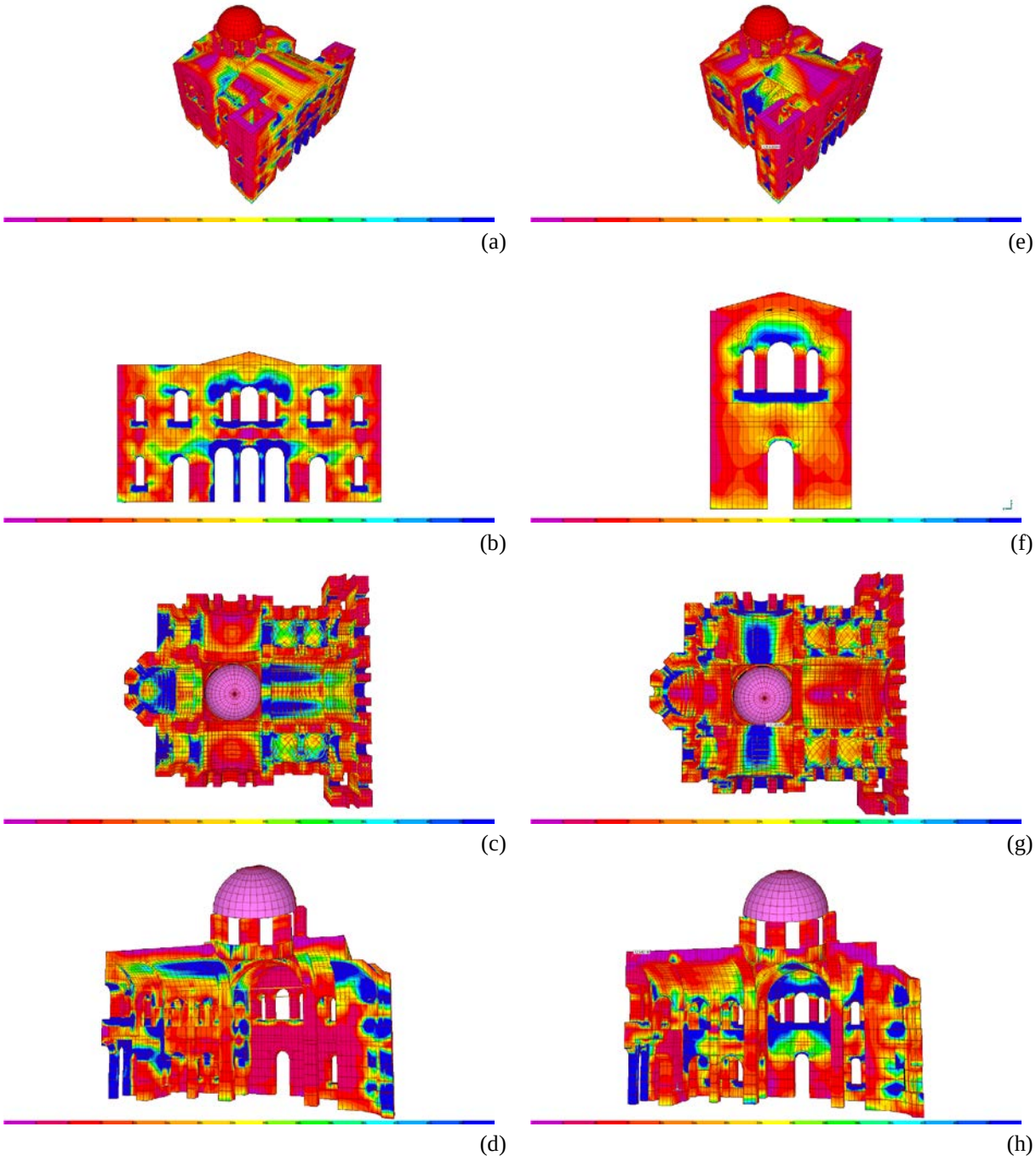

Figure-19: S11 (a-d) and S22 (e-h) stresses of the temple

Comparison between Tables 3 and 4 clearly indicates the anticipating decrease of the model periods of the strengthened structure after the interventions. According to the analysis excess of the compressive strength of the masonry does not appear after the consolidation of the walls with grout injections. Also, tensile stresses are smaller than the tensile strength attributed to the application of CFRP and tie rods. Excess of the tensile strength (10% of the tensile strength of the masonry) is limited at "secondary" places of the masonry walls for the seismic behavior and stability of the structure.

REFERENCES

[1] C.C. Spyrakos, *Finite Element Modeling in Engineering Practice*, Pittsburgh PA, 1994.

[2] Θ.Π. Τάσιος, Μ.Π. Χρονόπουλος, *Παθολογικά Αίτια και Μηχανική των Βλαβών της Τοιχοποιίας,* Υ.ΠΕ.ΧΩ.ΔΕ./ Εργ. Ωπλ. Σκυροδέματος Ε.Μ.Π., Αθήνα, 1986.

[3] SAP2000. Structural analysis program, advanced 14.1.0. Berkeley, California: Computers and Structures, Inc.; 2009.

[4] ENV 1998-1, Eurocode 8. Design of structures for earthquake resistance. Part1 General rules, seismic actions and rules for buildings. 2003. CEN.

[5] Κωνσταντίνος Σπυράκος, *Ενίσχυση Κατασκευών για Σεισμικά Φορτία*, Τεχνικό Επιμελητήριο Ελλάδας, Αθήνα, 2004.

[6] P. Foraboschi, *Strengthening of Masonry Arches with Fiber-Reinforced Polymer Strips*, J. Compos. Constr (ASCE), Vol. 8, No. 3, June 1, 2004.

[7] M.R. Valluzzi, F. da Porto, C. Modena, *Behavior and modeling of strengthened three-leaf stone masonry walls*, RILEM Materials and Structures, 37(267): 184-192, 2004.